Dyslipidemia-Induced Neuropathy in Mice
The Role of oxLDL/LOX-1

Andrea M. Vincent,[1] John M. Hayes,[1] Lisa L. McLean,[1] Anuradha Vivekanandan-Giri,[2] Subramaniam Pennathur,[2] and Eva L. Feldman[1]

OBJECTIVE—Neuropathy is a frequent and severe complication of diabetes. Multiple metabolic defects in type 2 diabetic patients result in oxidative injury of dorsal root ganglia (DRG) neurons. Our previous work focused on hyperglycemia clearly demonstrates induction of mitochondrial oxidative stress and acute injury in DRG neurons; however, this mechanism is not the only factor that produces neuropathy in vivo. Dyslipidemia also correlates with the development of neuropathy, even in pre-diabetic patients. This study was designed to explore the contribution of dyslipidemia in neuropathy.

RESEARCH DESIGN AND METHODS—Mice ($n = 10$) were fed a control (10% kcal %fat) or high-fat (45% kcal %fat) diet to explore the impact of plasma lipids on the development of neuropathy. We also examined oxidized lipid–mediated injury in cultured DRG neurons from adult rat using oxidized LDLs (oxLDLs).

RESULTS—Mice on a high-fat diet have increased oxLDLs and systemic and nerve oxidative stress. They develop nerve conduction velocity (NCV) and sensory deficits prior to impaired glucose tolerance. In vitro, oxLDLs lead to severe DRG neuron oxidative stress via interaction with the receptor lectin-like oxLDL receptor (LOX)-1 and subsequent NAD(P)H oxidase activity. Oxidative stress resulting from oxLDLs and high glucose is additive.

CONCLUSIONS—Multiple metabolic defects in type 2 diabetes directly injure DRG neurons through different mechanisms that all result in oxidative stress. Dyslipidemia leads to high levels of oxLDLs that may injure DRG neurons via LOX-1 and contribute to the development of diabetic neuropathy. *Diabetes* **58:2376–2385, 2009**

O ur work is focused on understanding the mechanisms that lead to diabetic neuropathy and developing rational therapeutic interventions. Hyperglycemia clearly leads to peripheral nerve injury through the development of systemic and neuronal oxidative stress (1–6). An emerging idea is that dyslipidemia also contributes to the development of diabetic neuropathy (7,8). Lipid profiles are commonly abnormal early in the course of type 2 diabetes in a temporal pattern that correlates with the presence of diabetic neuropathy, and we recently reported that elevated triglyceride levels predict a more rapid disease course (9,10). In addition, several large-scale trials of type 2 diabetic patients point to early dyslipidemia as a major independent risk factor for the development of diabetic neuropathy (11).

In experimental diabetes, the complex etiology of diabetic neuropathy is difficult to explore due to the multiple sources of nerve injury, including hyperglycemia, advanced glycation end products, systemic oxidative stress, and altered growth factor availability (12). Furthermore, lipid profiles of mice differ from human patients in that the majority of plasma cholesterol is transported in HDL and LDL levels are constitutively low (13). Mice with genetically increased plasma cholesterol have accelerated atherosclerosis that renders them unsuitable for neuropathy studies (13). Several studies (14–16) explored the role of a high-fat diet in the development of both diabetes and diabetic complications. Susceptibility to neuropathy is mouse strain dependent; the constitution of the diet is another important factor. One study (17) suggests that a high-fat diet produces neuropathy independent of hyperglycemia, and the present study explores a potential mechanism of high-fat–induced neuropathy.

Because high-fat diets increase plasma LDLs and pre-diabetes is associated with systemic oxidative stress (18), we proposed that oxidized LDLs (oxLDLs) will be elevated in mice fed a high-fat diet. Furthermore, we predicted that increased oxLDLs may produce dorsal root ganglia (DRG) neuron injury through binding the lectin-like oxLDL receptor (LOX)-1 in a similar manner to vascular endothelial cells (19) and renal tubular cells (20). The activation of LOX-1 on endothelial cells leads to intracellular oxidative stress and inflammation and a feed-forward cycle of injury in diabetes, since both oxLDLs and glucose increase LOX-1 expression (21,22).

In this study, we used high-fat feeding in the C57/BL6 mouse strain using a 45-kcal %fat (mostly from lard) diet. We demonstrate morphological and functional evidence of neuropathy prior to loss of glucose regulation in agreement with clinical findings (10,23,24). This is associated with significant increases in plasma oxLDLs. We assessed oxLDL-mediated injury in cultured DRG neurons from adult rats. oxLDLs directly lead to oxidative stress and injury in DRG neurons via LOX-1. DRG neuron injury is partially induced via activation of NAD(P)H oxidase. We conclude that diet-induced plasma oxLDLs can produce neuron injury and may be a contributing factor in the development of neuropathy in pre-diabetes or diabetes.

RESEARCH DESIGN AND METHODS

High-fat–fed mice. C57/BL6 mice (The Jackson Laboratory, Bar Harbor, ME) at 3 weeks of age were placed on either control AIN5003 (10% kcal %fat) or high-fat (45% kcal %fat) diet D12451i from Research Diets (New Brunswick,

TABLE 1
Oxidative stress measures in plasma, LDLs, and sciatic nerve

	Control mice	High-fat mice
HODE (pmol/mg protein)		
Plasma	97 ± 8	119 ± 6*
LDL cholesterol	116 ± 14	193 ± 10*
Sciatic nerve	117 ± 10	169 ± 16*
Dityrosine (μmol/mol tyrosine)		
Plasma	24 ± 2	36 ± 3*
LDL cholesterol	23 ± 2	546 ± 91*
Sciatic nerve	3 ± 1	8 ± 1*
Nitrotyrosine (μmol/mol tyrosine)		
Plasma	84 ± 8	147 ± 22*
LDL cholesterol	90 ± 11	144 ± 57*
Sciatic nerve	3 ± 1	17 ± 4*

Data are means $\pm$ SE. Lipid and protein peroxidation were assessed by reverse-phase high-performance liquid chromatography. HODE, dityrosine, and nitrotyrosine were all significantly increased in plasma ($n = 10$), sciatic nerve ($n = 10$), and isolated LDL ($n = 2$). *$P < 0.05$.

NJ), with 10 mice/group. Diets were matched for protein and carbohydrate content. Blood glucose was tested every 4 weeks following a 6-h fast. One drop of tail blood was analyzed using a standard glucometer (no. 6 strips, OneTouch Profile; Lifescan, Milpitas, CA). Glucose tolerance tests were performed by measuring blood glucose 5, 15, 30, 60, and 120 min after gavage administration of a glucose bolus. Nerve conduction velocity (NCV) studies were performed after 12 and 34 weeks and neuropathy phenotyping (see below) at termination at 34 weeks. GHb was measured using the Helena Laboratories test kit, Glyco-Tek Affinity Column Method (catalog no. 5351), as previously described (25,26). Insulin was measured by radioimmunoassay in the Michigan Diabetes Research and Training Center (MDRTC) Chemistry Core.

Nerve conduction studies. Hindpaw thermal latency and NCV were measured per our published protocols (2,12,26–28) and in compliance with protocols established by the Animal Models of Diabetic Complications Consortium (http://www.amdcc.org). Mice were anesthetized with 30/0.75 mg/kg ketamine/acepromazine by peritoneal injection, and body temperatures were maintained at 32–34°C using a heating pad.

Tissue harvest. Mice were killed with an overdose of pentobarbital 34 weeks after initiation of control or high-fat diet. Sciatic nerves were harvested and submerged in ice-cold antioxidant buffer A (100 μmol/l diethylene tetramino pentaacetic acid, 50 μmol/l butylated hydroxyl toluene, 1% [vol/vol] ethanol, 10 mmol/l 3-amino-1,2,4-triazole, and 50 mmol/l sodium phosphate buffer, pH 7.4), rapidly frozen by immersion in liquid nitrogen, and stored at −80°C until analysis. A blood sample (100–300 μl) was collected into K_3 EDTA vacutainer tubes (Becton Dickinson, Franklin Lakes, NJ) and centrifuged at 100g for 15 min at 4°C. Plasma was collected and stored at −80°C.

Intraepidermal nerve fiber density. Foot pads were collected from the hindpaw plantar surface; postfixed in Zamboni's (2% PFA, 1% picric acid in 0.1 mol/l PBS) solution overnight; rinsed in 5, 10, and 20% sucrose in 50 mmol/l sodium phosphate buffer; cryoembedded; sectioned (35 μm); and processed for PGP 9.5 immunohistochemistry (1:2,000; Chemicon, Temecula, CA) per our previous work (25,26,28). The data are presented as the number of fibers per millimeters squared across one entire papilla.

Plasma lipid profiling. Plasma samples from five mice per group were pooled to produce two pools per group, and each pool was run five times on fast-protein liquid chromatography then the fractions assayed for cholesterol and triglycerides. These assays were performed as previously published by the Mouse Metabolic Phenotyping Center Core at the University of Washington, Seattle (29). LDLs were isolated from mouse plasma by discontinuous density ultracentrifugation as described previously (30). A total of 200 μl plasma was overlaid with normal saline ($d = 1.006$ kg/l) and ultracentrifuged for 60 min at 541,000g_{max} at 4°C. After removal of VLDLs from the top, the density was adjusted with solid KBr to $d = 1.300$ kg/l, then overlaid with normal saline and ultracentrifuged for 60 min at 541,000g_{max} at 4°C. LDLs were removed by aspiration of the top layer. The sample was desalted using a PD10 column (Sephadex G-25M; Amersham) and eluted with 0.01 mol/l PBS (pH 7.4).

Hydroxyoctadecadienoic acid, dityrosine, and nitrotyrosine levels. Hydroxyoctadecadienoic acid (HODE), dityrosine, and nitrotyrosine were measured in plasma, sciatic nerve, and isolated LDLs, as described previously (31–33). HODEs were quantified in lipid extracts by reverse-phase C-18
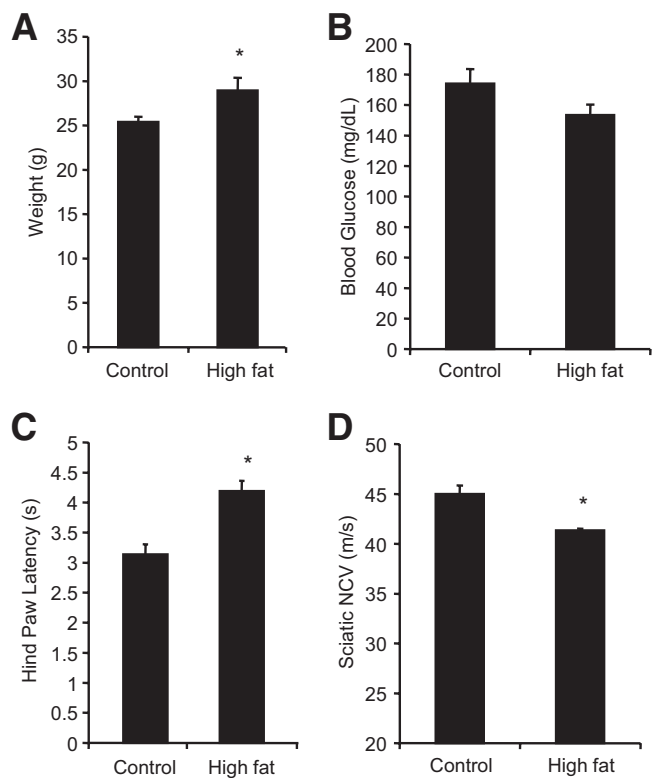

FIG. 1. Mild neuropathy after 12 weeks of high-fat diet. Following 12 weeks of high-fat or control diet, weight (A), blood glucose (B), hindpaw withdrawal latency (C), and sciatic NCV (D) were assessed. $n = 10$/group. *$P < 0.05$ vs. control diet.

high-performance liquid chromatography (250 $\times$ 4.6 mm, particle size 5 μm, Ultrasphere column; Beckman). Amino acids were analyzed by reverse-phase high-performance liquid chromatography (Jasco HPLC column, C-18 column 250 $\times$ 4.6 mm, particle size 5 μm, ODS Ultrasphere; Beckman). The identity and quantity of the compounds were confirmed by identical retention time on standard curves with authentic o,o'-dityrosine and tyrosine by monitoring absorbance at 460 nm. Nitrotyrosine was quantified by isotope dilution mass spectrometry as described previously (33).

Adult DRG neuron cultures. DRG were collected from killed adult female Sprague-Dawley rats and dissociated in 0.2% collagenase for 30 min followed by 1% trypsin for 15 min. Cells were seeded on collagen-coated plates in DMEM:F-10, 50:50, containing 1 $\times$ B27 additives, 40 μmol/l 2'-Deoxy-5-fluorouridine (FUDR), 7 μmol/l aphidicolin, and 1,000 units/ml penicillin/streptomycin/neomycin. Cells were refed on day 2, and experiments were performed on day 3. In this media, the basal glucose concentration is 5.7 mmol/l. For high-glucose experiments, 20 mmol/l glucose is added to the media, yielding a total of 25.7 mmol/l. For oxLDL experiments, a dose curve from 1 to 100 μg/ml was selected, based on other in vitro studies (34–37). From LDL isolation, we estimate that there was ~300–400 μg/ml LDL protein in the mouse plasma. The amount of LDL protein was not significantly different between control and high-fat mice, but oxidation markers were 1.6- to 24-fold higher in high-fat compared with control mice (Table 1). This plasma LDL concentration is 10–30 times higher than the 30 μg/ml dose oxLDL used in the in vitro experiments. Control experiments were always performed with nonoxidized LDLs, and these did not produce the cellular responses of oxLDLs (data not shown).

Measurement of reactive oxygen species. MitoSOX and dihydroethidium (DHE) (Molecular Probes, Eugene, OR) are cell-permeable probes that fluoresce in the presence of superoxide. The probes are used as previously described (25,38,39). Mean red fluorescence per well is read at 485 nm excitation and 590 nm emission (Fluoroskan Ascent II plate reader; LabSystems, Helsinki, Finland).

Total radical antioxidant potential. Total radical antioxidant potential (TRAP) is determined by a luminometric method per our published protocols (1,25). DRG neurons were lysed in ultrapure water and tested for the ability to prevent 2,2'-azobis(amidinopropane) dihydrochloride (ABAP)-induced luminescence in the presence of electrochemiluminescence reagent (Amersham, PA). The data were normalized to the untreated control samples (100%).
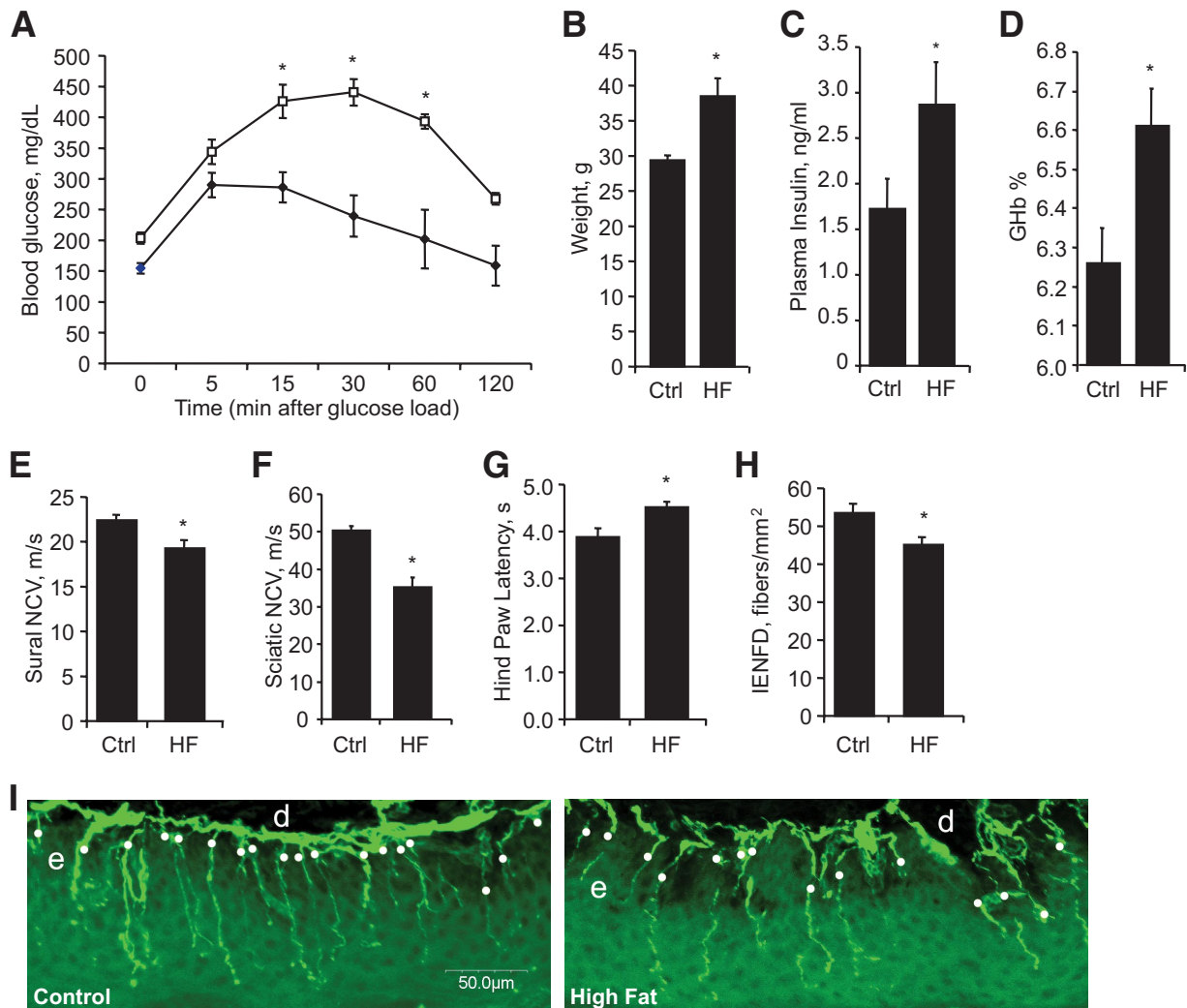
FIG. 2. Neuropathy and impaired glucose tolerance after 34 weeks on high-fat diet. Complete phenotyping after 34 weeks on control (Ctrl) or high-fat (HF) diet was performed. The figure displays the glucose tolerance test (*A*), weight (*B*), plasma insulin (*C*), GHb (*D*), sural NCV (*E*), sciatic NCV (*F*), hindpaw withdrawal latency (*G*), and IENFD (*H*). *$P < 0.05$ vs. the control diet group. In all panels, $n = 10$. *A*: ♦, control; □, high fat. *I*: Representative IENFD images from one control-fed and one high-fat–fed sample. Bar = 50 μm; d = dermis, e = epidermis. White dots indicate nerve fibers counted. (A high-quality digital representation of this figure is available in the online issue.)

NAD(P)H oxidase activity. NAD(P)H oxidase activity in DRG neuron lysates is assessed as previously described (1). The rate of luminescence increase in the presence or absence of apocynin was calculated to give a measure of superoxide generation by NAD(P)H oxidase activity (luminescence units/min).

Fragmentation of genomic DNA. TdT-mediated dUTP-biotin nick-end labeling (TUNEL) staining is used to detect cell death in cultured DRG neurons (10,18,29). Samples are fixed in 4% paraformaldehyde, labeled with digoxygenin-dUTP, then stained with horseradish peroxidase–conjugated anti-digoxygenin antibody using a kit according to the manufacturer's instructions (Intergen, Gaithersburg, MD).

Immunohistochemistry. DRG neurons were fixed in 4% paraformaldehyde in 0.1 mol/l PBS solution for 5 min. Primary antibodies were applied in 0.1 mol/l PBS/1% Triton × 100/5% serum for 16 h at 4°C. Cells were washed for 3 × for 10 min each in PBS, and then species-specific secondary antibody was conjugated to AlexaFluor 594, (Molecular Probes, Eugene, OR) diluted 1:1,000 in 0.1 mol/l PBS containing 1% Triton × 100 and 5% serum. After a further 1 h at room temperature, cells were washed 3 × for 10 min each in PBS. For nitrotyrosine, the primary was antibody 244 (10 μg/ml; Upstate Biologicals, Lake Placed, NY). Fluorescence was quantitated in the fluorescent plate reader at 485 excitation and 590 emission. For LOX-1, the primary was Ox-LDL R-1 (Y-21), from Santa Cruz sc11653, diluted 1:100. Immunofluorescence was examined on an Olympus Fluoview inverted microscope.

Western blotting. Western blotting was performed per our previous studies (1–3) with 40 μg protein/lane, separated on a 12.5% polyacrylamide gel.

Caspase 3. After 5-h exposure to 20 mmol/l excess glucose, one coverslip from each dose was treated with fluorescent CaspaTag reagent per manufac-

turer's protocol (Chemicon, San Francisco, CA) and assessed in the fluorescence plate reader per previous studies (1,25).

Statistical analysis. In cell culture studies, all experimental paradigms were performed in triplicate on three separate occasions with different cell cultures, giving a final $n = 9$ for each data point. In mouse studies, there were 10 mice per group for all in vivo studies. Lipid profiling was performed three times on each of two pools of plasma per group ($n = 2$). Data analyses were performed using Prism, version 3 (GraphPad Software). Assumptions about the Gaussian distribution of data and rules for transformation of nonnormative data were made as previously described (28). Comparison of dependent variables was performed using factorial ANOVA with 95% CIs. All measurements were made by an observer blinded to the experimental condition. Bar graphs illustrate the mean ± SE.

RESULTS

High-fat–fed mice develop neuropathy. Following 12 weeks on a high-fat diet, mice were modestly heavier than mice on a control diet (28.9 ± 1.4 g compared with 25.4 ± 0.5 g) (Fig. 1*A*) but did not have increased fasting blood glucose (Fig. 1*B*). Despite the lack of evidence for glucose intolerance, the mice displayed evidence of neuropathy. The latency of hindpaw response to a heat stimulus was significantly increased ($P < 0.05$) (Fig. 1*C*), and the sciatic NCV was slowed in the high-fat mice ($P < 0.05$) (Fig. 1*D*).
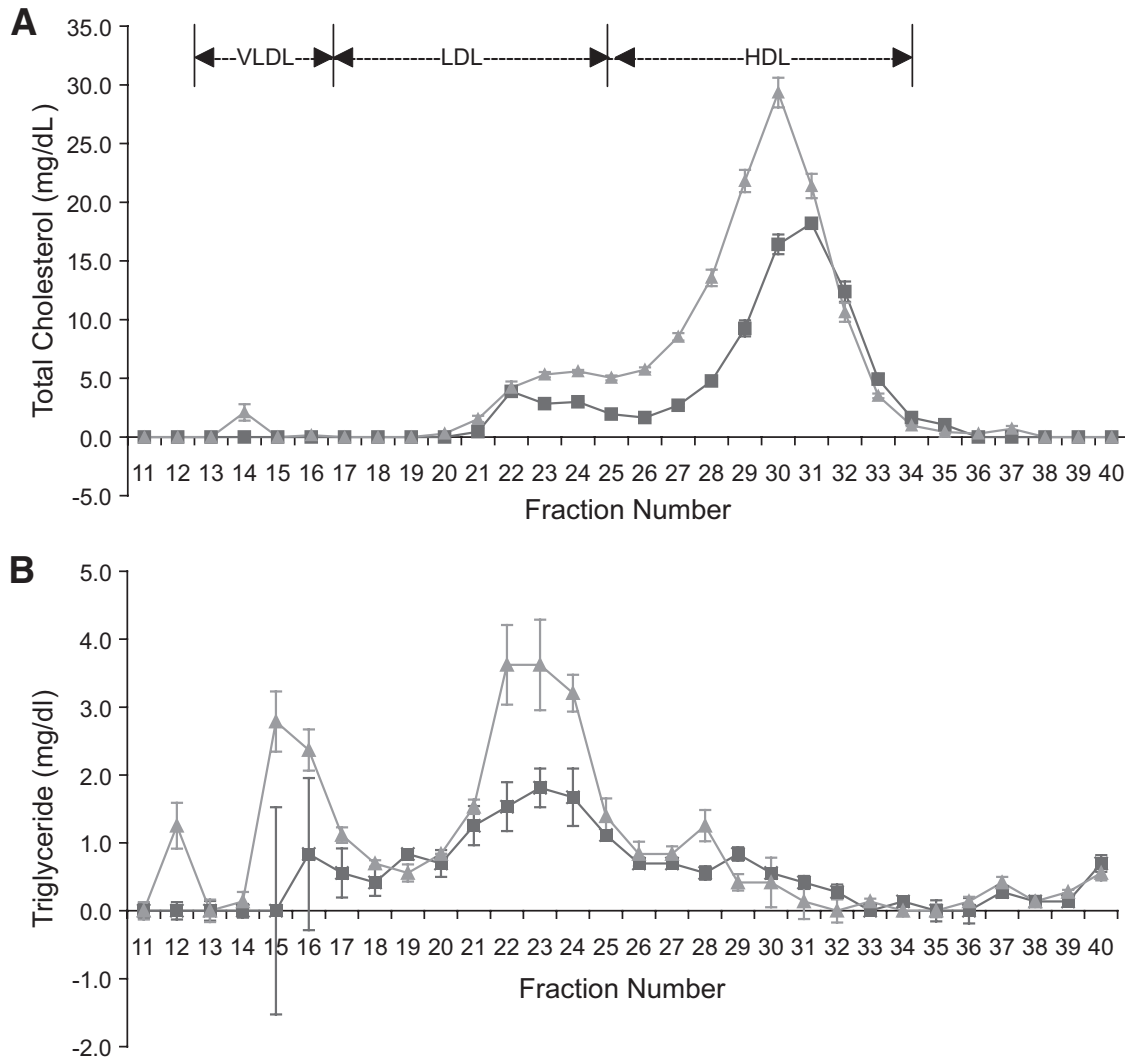
FIG. 3. Plasma lipid profiles in the plasma at 34 weeks. Pooled plasma samples (two pools per group, each pool analyzed three times) were subjected to fractionation by FPLC; then cholesterol (*A*) and triglycerides (*B*) were measured in each fraction. The graph shows the means ± SE for *n* = 2 pools/group. ■ regular diet; ▲, high-fat diet.

Other neuropathy measures at 12 weeks (tail flick and sural NCV) showed no difference between control and high-fat diet–fed mice (not shown).

By 34 weeks, mice displayed glucose intolerance with significantly higher blood glucose levels 15 min after applying the glucose bolus, and this difference remained at 2 h (Fig. 2*A*). Similarly, body weight, plasma insulin, and GHb were all significantly increased in the high-fat group compared with those on the control diet (Fig. 2*B–D*), indicating frank diabetes in the high-fat mice. NCV measures in sural ($P < 0.05$) and sciatic ($P < 0.01$) nerves were both decreased in the high-fat mice compared with control diet mice (Fig. 2*E–F*). Sensory neuropathy was evident in the high-fat mice through decreased response to a heat stimulus on the hindpaw (Fig. 2*G*) and decreased intraepidermal nerve fiber density (IENFD) in the hindpaw skin (Fig. 2*H–I*).

Oxidative stress was assessed in plasma, isolated LDLs, and sciatic nerves (Table 1). Plasma lipids were significantly oxidized, as evidenced by increased HODE, and plasma proteins were both oxidized (dityrosine) and nitrosylated (nitrotyrosine) in high-fat–fed mice compared with mice on the control diet. We also measured these oxidation markers in LDLs isolated from the mice to confirm the elevation of oxLDLs (Table 1). Next, we compared plasma lipid profiles between the two groups of mice. HDL were increased and the peak shifted slightly left in the high-fat–fed group, indicating uptake of cholesterol. There was also a shift in the high-fat–fed group to increase the population of LDLs, and these contain significantly elevated triglycerides. Also, a peak of VLDLs is evident in the high-fat mice but absent in the control diet mice (Fig. 3*A*). There were significant increases in the levels of triglycerides associated with the LDL/VLDL samples in the high-fat–fed mice, as well as free triglycerides in the high-fat–fed mice only (Fig. 3*B*). Together, data in Table 1 and Fig. 3 confirm that high-fat feeding increases plasma lipids and oxLDLs.

DRG neurons express LOX-1. We demonstrated that DRG neurons express the receptor for oxLDL, LOX-1, by immunocytochemistry and Western blotting. The Western blot demonstrates that three isoforms of LOX-1 are present in adult DRG neurons (Fig. 4*A*). The 48-kDa glycosylated form is most highly expressed in the neurons. This isoform is glycosylated for transport to the plasma membrane and is considered the active isoform (40).
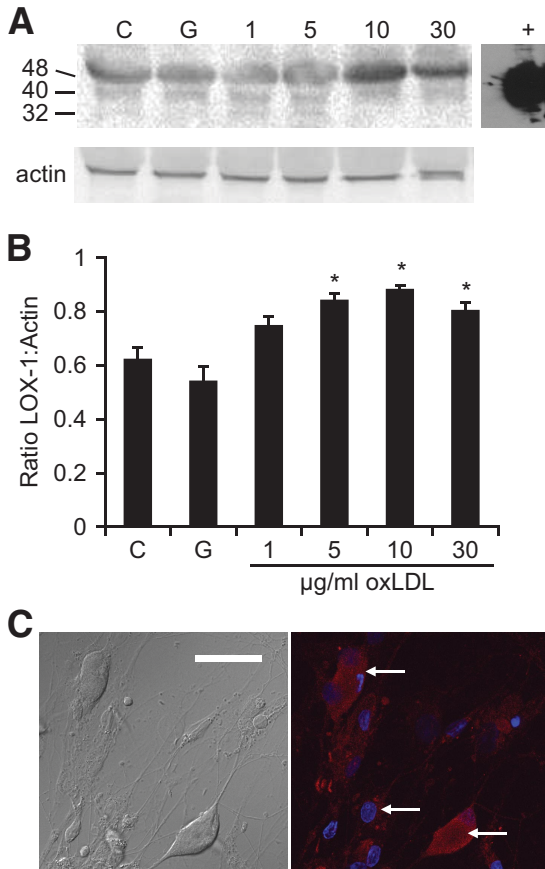
FIG. 4. LOX-1 expression on DRG neurons. DRG neurons from adult rat were assessed for LOX-1 by Western blotting (*A* and *B*) and immunocytochemistry (*C*) after 3 days in culture. *A*: A total of 40 μg protein from untreated control (C) cultures in *lane 1* display the glycosylated 48-kDa isoform of LOX-1 that is predicted to be at the cell surface. The lower–molecular weight precursor (40 kDa) and nonglycosylated (32 kDa) isoform are also present. Exposure to high glucose (G) (20 mmol/l added, total 25.7 mmol/l glucose) or 1 μg/ml oxLDL for 3 h did not alter LOX-1 expression. A total of 5, 10, or 30 mg/ml oxLDL for 3 h increased the level of the 48-kDa isoform, and the two higher doses appear to decrease the lower–molecular weight forms. +, a positive control peptide based on the 40 kDa predicted precursor form of LOX-1. *B*: Densitometry was performed on three replicates of the representative blot shown in *A*. Mean pixel densities for the 48-kDa band are normalized against actin. The graph shows the means ± SE. *$P < 0.05$ vs. the untreated control. *C*: A representative image of untreated DRG neurons is shown. White arrows indicate neurons labeled for LOX-1. Bar = 50 μm. (A high-quality digital representation of this figure is available in the online issue.)

Exposure to ≥5 μg/ml concentrations of oxLDLs for 3 h led to an increase in the 48-kDa isoform (Fig. 4*B*). Immunocytochemistry in control DRG neurons confirms that LOX-1 is present on the neurons (*arrows*) and not only on residual Schwann cells in the cultures (Fig. 4*C*).

oxLDLs generate oxidative stress in DRG neurons via LOX-1. To define the mechanisms of oxidized lipid–induced neuropathy, we explored the effects of oxLDLs on adult DRG neurons in culture. We found a dose-dependent increase in mitochondrial superoxide after a 1-h exposure to oxLDLs (Fig. 5*A*). Above 30 μg/ml oxLDLs there was a significant increase in mitochondrial superoxide that was additive to the levels produced by high glucose. Using a second probe, DHE, we confirmed that a portion of oxLDL-induced superoxide involved the mitochondria (Fig. 5*B*). We demonstrate that, similar to MitoSOX oxidation, DHE oxidation increases above 30 μg/ml oxLDL and that ~50% of this signal is blocked in the presence of the

mitochondrial uncoupler carbonylcyanide-*p*-trifluoromethoxyphenylhydrazone (FCCP) (2.5 μmol/l). This dose of FCCP leads to loss of mitochondrial membrane potential and ATP generation, and the data suggest that ~50% of the DHE signal is produced via mitochondrial electron transfer chain generation of superoxide. Preloading the cells with α-lipoic acid (100 μmol/l) also blocked DHE oxidation at 10 and 30 μmol/l doses. α-Lipoic acid decreased ($P < 0.05$) but did not completely prevent DHE oxidation in response to 100 μmol/l oxLDL (Fig. 5*B*). Confirmation that generation of superoxide leads to oxidative stress in this system was achieved using assays for TRAP (Fig. 5*C*) and cellular nitrotyrosine (Fig. 5*D*). Using a single dose and time point where there was substantial oxidative stress in the MitoSOX assay, exposure to 30 μg/ml oxLDL for 3 h significantly decreased the antioxidant potential of DRG neurons by >40%. Doses as low as 10 μg/ml oxLDL increased nitrotyrosine over 24 h in the DRG neurons (Fig. 5*D*), and 100 μg/ml oxLDL achieved nitrotyrosine levels similar to high glucose. oxLDL-induced, but not high-glucose–induced, nitrotyrosine was blocked by preincubating the DRG neurons with a LOX-1 neutralizing antibody (100 mg/ml).

oxLDL-/LOX-1–induced DRG neuron injury involves NAD(P)H oxidase. We next examined DRG neuron injury via activation of caspase 3 (Fig. 6*A*) and degradation of nuclear DNA (Fig. 6*B*). Activation of caspase 3 after 5 h was significantly increased by at least threefold in the presence of high glucose or 10, 30, or 100 μg/ml oxLDL. Pretreatment with LOX-1 neutralizing antibody (100 mg/ml) significantly blocked oxLDL-induced, but not glucose-induced, caspase 3 activation. The NAD(P)H oxidase inhibitor apocynin (1 μmol/l) significantly blocked caspase 3 activation with 10 μg/ml oxLDL but decreased with increasing concentrations of oxLDLs. This may be due to the dose of apocynin being too low to block high levels of NAD(P)H oxidase activity, but higher doses of apocynin induce oxidative stress and cell injury (data not shown). The antioxidant α-lipoic acid (100 μmol/l) efficiently blocked caspase 3 activation induced by both high glucose and doses of oxLDLs up to 100 μmol/l.

The TUNEL assay was performed after 24 h to determine the total cell death caused by high-glucose or oxLDL treatments. High glucose produces 60 ± 4% DRG neuron death after 24 h (Fig. 6*B*). This death is completely blocked by the antioxidant α-lipoic acid (100 μmol/l), consistent with high-glucose injury in these cells via mitochondrial oxidative stress, as we previously published in embryonic DRG (Fig. 4*A*). Glucose-induced injury was not altered by anti–LOX-1 or by apocynin.

At 10 μg/ml oxLDL, there was an ~10% increase in TUNEL over 24 h. There was no significant effect of antioxidant or apocynin, but blocking LOX-1 significantly decreased TUNEL to control levels (Fig. 6*B*). A total of 30 μg/ml oxLDL increased TUNEL to ~60% and 100 μg/ml to 70%. All three inhibitors—apocynin, anti–LOX-1, and antioxidant—significantly decreased oxLDL-induced cell death to approaching control levels ($P < 0.01$).

Confirmation that oxLDL/LOX-1 interaction activates NAD(P)H oxidase. Next, we examined the activation of NAD(P)H oxidase at the 1- and 3-h time points (Fig. 7). Both p47 and gp91 were localized in the cell soma in untreated control DRG neurons, but 3 h subsequent to exposure to oxLDLs, labeling was also identified along the dendrites and the intensity of staining was increased (Fig. 7*A*). The activity of NAD(P)H oxidase was significantly
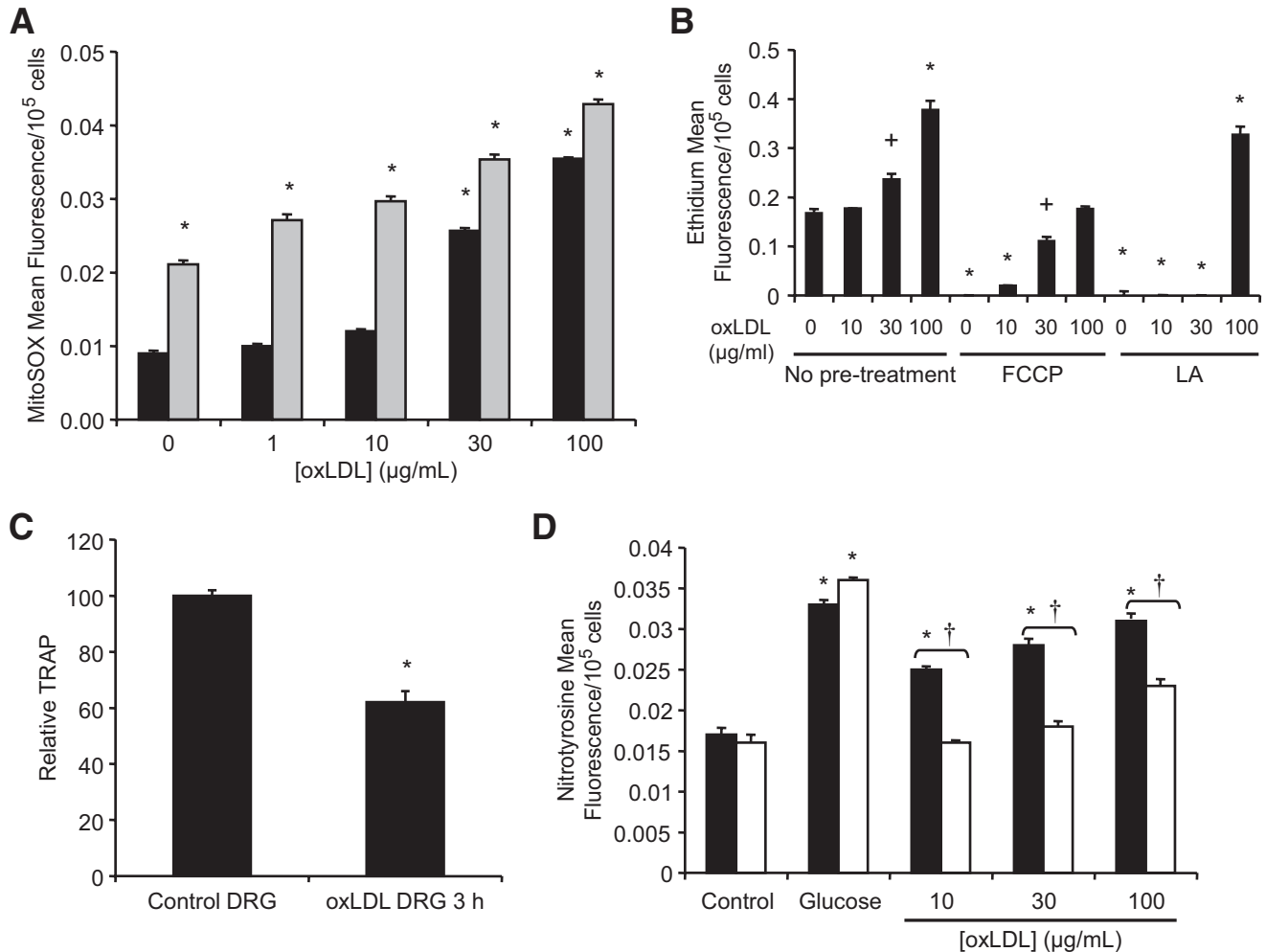
FIG. 5. High glucose and oxLDL induce oxidative stress in adult DRG neurons. After 3 days in culture, oxidative stress assays were performed in cultured DRG neurons. *A*: DRG neurons were exposed to increasing concentrations of oxLDL in the presence of basal (5.7 mmol/l) or high (25.7 mmol/l) glucose for 1 h, then loaded with MitoSOX for 15 min. $n = 9$, *$P < 0.01$ vs. control (basal glucose, 0 μg/ml oxLDL). ■, basal glucose; ▨, high glucose. *B*: DRG neurons were exposed to increasing concentrations of oxLDL alone or in the presence of the mitochondrial uncoupler FCCP (2.5 μmol/l) or the antioxidant α-lipoic acid (LA) (100 μmol/l) for 1 h, then loaded with DHE for 15 min. $n = 9$; *$P < 0.01$, +$P < 0.05$ vs. control. *C*: TRAP was assessed in untreated DRG neurons and those exposed to 30 μg/ml oxLDL for 3 h, $n = 3$, *$P < 0.01$. *D*: Nitrotyrosine fluorescence was assessed 24 h following exposure to high glucose or increasing concentrations of oxLDL in the presence or absence of LOX-1–neutralizing antibody (100 mg/ml). ■, none; □, anti–LOX-1. $n = 9$, *$P < 0.01$ vs. untreated control; †$P < 0.01$ vs. no antibody.

increased after 1- and 3-h exposure to high glucose, as we showed previously (1). Following exposure to 30 μg/ml oxLDL, NAD(P)H oxidase activity increased by ~100% but was decreasing toward control levels by 3 h (Fig. 7*B*). By Western blotting, the p47 subunit was increased in DRG neurons exposed to high glucose or oxLDLs (30 μg/ml) for 3 h. The gp91 antibody did not produce a clearly defined band on Western blots (not shown).

DISCUSSION

In this report, we confirm that high-fat feeding in mice produces neuropathy and increased tissue and systemic oxidative stress prior to the development of frank diabetes. We postulated that these metabolic changes would generate oxLDLs and that these could contribute to neuronal injury mechanisms. We demonstrate that DRG neurons express the oxLDL receptor LOX-1 and that activation of this receptor in vitro leads to NAD(P)H oxidase activity that injures DRG neurons via generation of oxidative stress.

After 12 weeks on a high-fat diet, weight was modestly increased while fasting blood glucose remained normal.

The hindpaw latency was increased and sciatic NCV decreased, consistent with peripheral neuropathy. Previous studies (14,41,42) established that a high-fat diet leads to type 2 diabetes in mice. These studies focused on the mechanisms leading to insulin resistance, although one study (43) examined the consequences of a high-fat diet on the onset of nephropathy and one (17) on neuropathy. No previous study has shown that a high-fat (specifically high cholesterol) diet leads to NCV deficits and reduced hindpaw withdrawal response prior to impaired glucose tolerance. Our current data suggest that high-fat–induced neuronal deficits may precede the development of diabetes.

By 34 weeks on the high-fat diet, the mice displayed impaired glucose tolerance, a significant increase in plasma insulin levels, and an increase in GHb. These increases are small compared with mice with frank type 2 diabetes, where the plasma insulin may be elevated four-fold and GHb by several percent, but the extent of neuropathy is comparable (26). This provides supporting evidence for a role for dyslipidemia in the development of neuropathy. Clinical studies support this finding. In the
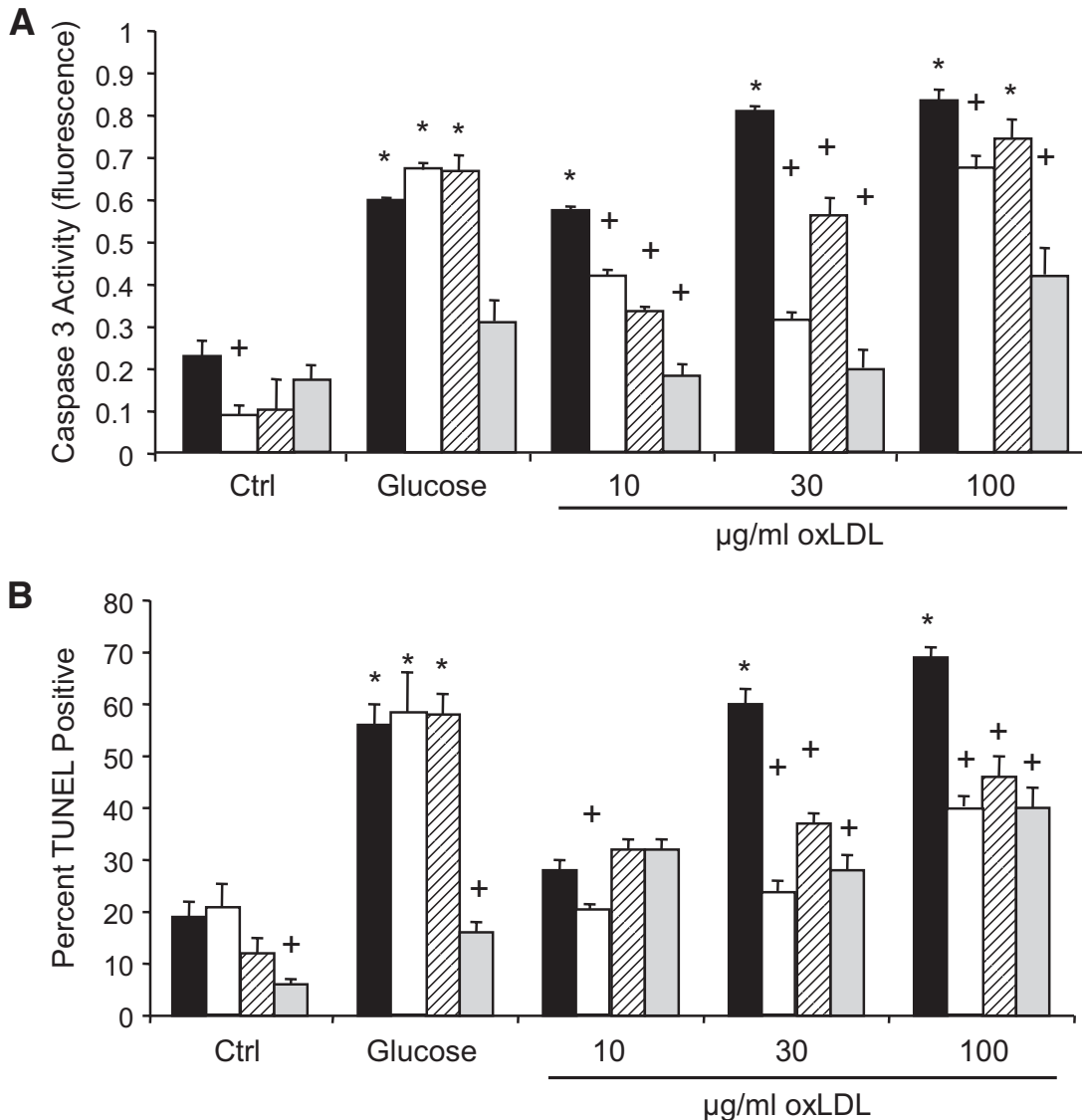
FIG. 6. High glucose and oxLDL cause cell death in DRG neurons. Adult DRG neurons were exposed to high glucose (25.7 mmol/l) or increasing concentrations of oxLDL, and then cell death was quantitated by caspase 3 activation after 5 h (*A*) or TUNEL after 24 h (*B*). DRG neurons were additionally pretreated with LOX-1–neutralizing antibody (□, 100 mg/ml), apocyanin (▨, 1 μmol/l), or α-lipoic acid (▦, 100 μmol/l). $n = 9$, *$P < 0.01$ vs. untreated control, +$P < 0.01$ vs. no pretreatment (■, None).

EURODIAB trial, of 1,200 subjects who did not have diabetic neuropathy at baseline, hypertension, serum lipids, and BMI were each independently associated with the risk of developing diabetic neuropathy during a 7-year follow-up period. Of these risk factors, dyslipidemia was closely linked with the onset and progression of diabetic neuropathy (44). In parallel, we recently reported that dyslipidemia, not hyperglycemia, was more closely correlated with neuropathy progression in 427 trial participants (10).

We demonstrate not only that the high-fat diet produced dyslipidemia, with high levels of HDL and LDL cholesterol and triglycerides, but also that LDLs and other circulating lipids and proteins are oxidized. Oxidatively modified proteins and lipids are toxic to complication-prone tissues, such as renal tubules (20) and the retina (45). In particular, oxLDLs mediate vascular injury via interaction with LOX-1 on endothelial cells (46). This led us to postulate that oxLDLs may injure DRG neurons.

We report strong expression of LOX-1 on the adult DRG

neurons by Western blotting and immunocytochemistry. Next, we characterized the effects of high glucose and oxLDLs on DRG neuron oxidative stress. Both insults lead to mitochondrial superoxide formation, the key mediator of DRG neuron injury in high glucose (1,2,38,47). The effects of high glucose and oxLDLs on mitochondrial superoxide were additive. Furthermore, antioxidant potential is depleted over time by oxLDLs. Using a neutralizing antibody to LOX-1, we demonstrate that the effects of oxLDLs are largely mediated via the LOX-1 receptor. This protection has been shown for vascular injury in dyslipidemia (48) but not previously for neurons. Our data suggest that multiple metabolic deficits in dyslipidemia and early diabetes combine to produce oxidative stress and accelerate the onset and progression of neuropathy. These data strongly argue for an antioxidant component to therapies for diabetic neuropathy (49). Our work also raises the interesting question of how obesity, immobility, and the metabolic syndrome contribute to neuropathy.

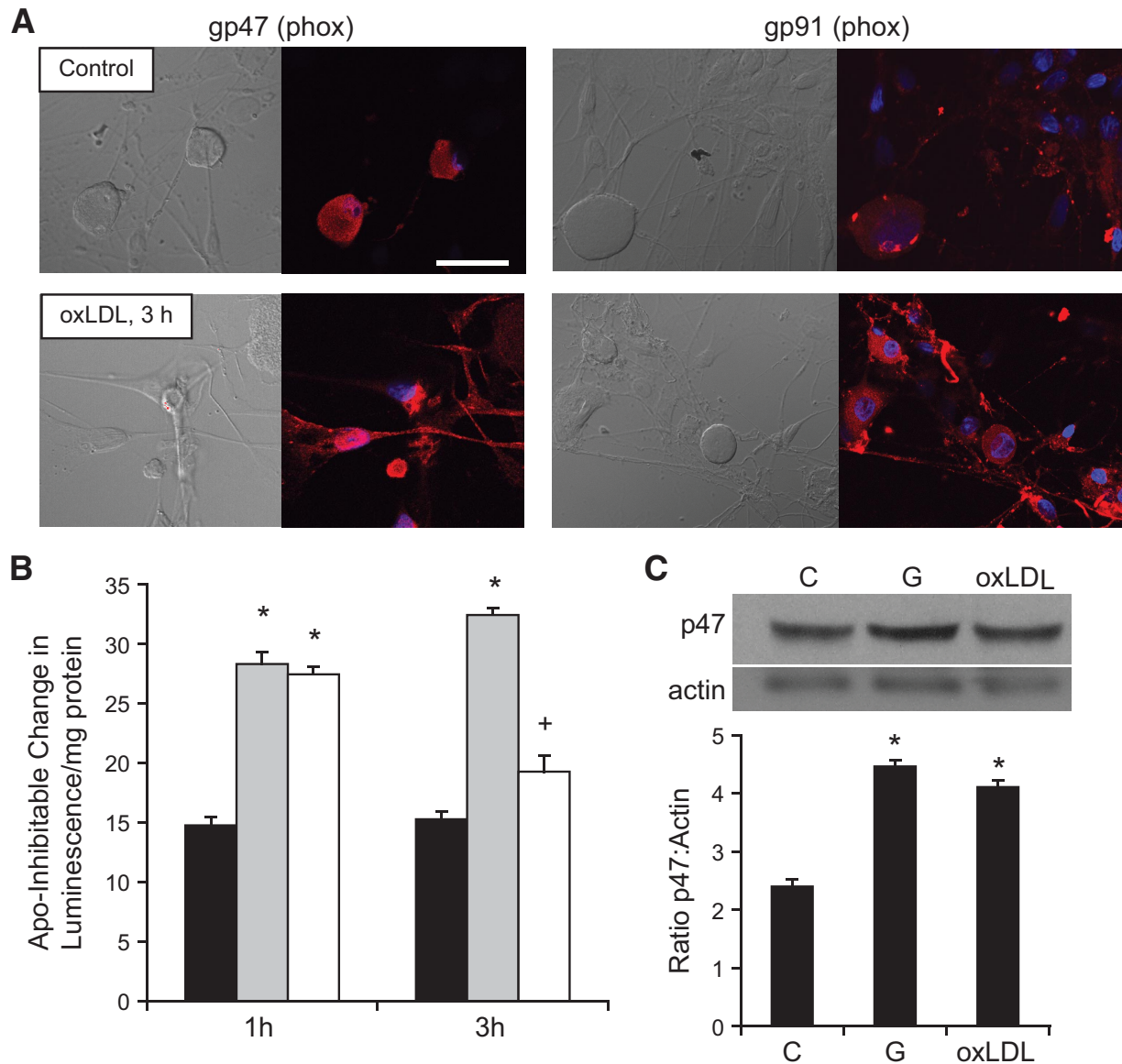High glucose or oxLDLs insults increased DRG neuron

FIG. 7. High glucose and oxLDL activate DRG neuron NAD(P)H oxidase. *A*: Adult DRG neurons were exposed to 30 μg/ml oxLDL and then immunolabeled for NAD(P)H oxidase subunits p47 or gp91. *B*: Adult DRG neurons were exposed to high glucose (25.7 mmol/l) or oxLDL (30 μg/ml) for 1 or 3 h, then lysed for biochemical assays of NAD(P)H oxidase. *$P < 0.01$ vs. untreated control, $+P < 0.05$ vs. untreated control. ■, control; ▨, glucose; □, oxLDL. *C*: Adult DRG neurons were exposed to high glucose (G) (25.7 mmol/l) or oxLDL (30 μg/ml) for 3 h then lysed for Western blotting. The representative image shows the immunoblot for p47 and the loading control actin, and the bar graph contains the means ± SE of three repeats of the illustrated blot. *$P < 0.01$ vs. untreated control (C). (A high-quality digital representation of this figure is available in the online issue.)

injury, evidenced by the activation of caspase 3 and by nuclear DNA degradation. The injury produced by either stressor was blocked by the antioxidant α-lipoic acid. These data support the consensus that pathways leading to cellular injury in diabetes (mainly shown for hyperglycemia to date) converge upon oxidative stress. Antioxidant therapies remain the most promising strategy for diabetic neuropathy, but clearly greater understanding of the long-term application of antioxidant therapy needs to be explored.

We also found that inhibition of NAD(P)H oxidase could block oxLDL-induced, but not high-glucose–induced, injury. Supporting evidence that oxLDLs led to NAD(P)H oxidase activity was obtained by observing subunit expression and localization and by measuring apocyanin-inhibitable NADPH oxidation. Thus, NAD(P)H oxidase activation and subsequent generation of superoxide is the primary injury mechanism in oxLDL-treated DRG neurons. This activation of NAD(P)H oxidase is mediated via LOX-1 signaling, since blocking LOX-1 abrogates oxLDL-induced DRG neuron injury. Our data agree with studies showing LOX-1–mediated activation of NAD(P)H oxidase in vascular endothelial cells through recruitment of NAD(P)H oxidase subunits (50). Collectively, these data demonstrate a pivotal role for NAD(P)H oxidase in the injury of DRG neurons and the progression of neuropathy (51).

This study demonstrates a mechanism by which dyslipidemia produces DRG neuron injury that may underlie emerging clinical evidence that dyslipidemia is an independent risk factor for diabetic neuropathy. The data suggest why glycemic control alone is insufficient to prevent complications in type 2 diabetes and argue for combination therapies targeting multiple metabolic imbalances and receptor-mediated signaling that leads to oxidative injury.

Prevention of oxLDL formation may be one strategy, but targeting oxLDL receptors may be an important alternative approach.

REFERENCES

1. Vincent AM, Perrone L, Sullivan KA, Backus C, Sastry AM, Lastoskie C, Feldman EL. Receptor for advanced glycation end products activation injures primary sensory neurons via oxidative stress. Endocrinology 2007;148:548–558
2. Vincent AM, McLean LL, Backus C, Feldman EL. Short-term hyperglycemia produces oxidative damage and apoptosis in neurons. FASEB J 2005;19:638–640
3. Vincent AM, Olzmann JA, Brownlee M, Sivitz WI, Russell JW. Uncoupling proteins prevent glucose-induced neuronal oxidative stress and programmed cell death. Diabetes 2004;53:726–734
4. Low PA, Nickander KK, Tritschler HJ. The roles of oxidative stress and antioxidant treatment in experimental diabetic neuropathy. Diabetes 1997;46(Suppl. 2):S38–S42
5. Osawa T, Kato Y. Protective role of antioxidative food factors in oxidative stress caused by hyperglycemia. Ann N Y Acad Sci 2005;1043:440–451
6. Tomlinson DR, Gardiner NJ. Glucose neurotoxicity. Nat Rev Neurosci 2008;9:36–45
7. Cameron NE, Cotter MA. Pro-inflammatory mechanisms in diabetic neuropathy: focus on the nuclear factor kappa B pathway. Curr Drug Targets 2008;9:60–67
8. Leiter LA. The prevention of diabetic microvascular complications of diabetes: is there a role for lipid lowering? Diabetes Res Clin Pract 2005;68(Suppl. 2):S3–S14
9. Meyer C, Milat F, McGrath BP, Cameron J, Kotsopoulos D, Teede HJ. Vascular dysfunction and autonomic neuropathy in type 2 diabetes. Diabet Med 2004;21:746–751
10. Wiggin TD, Sullivan KA, Pop-Busui R, Amato A, Sima AA, Feldman EL. Elevated triglycerides correlate with progression of diabetic neuropathy. Diabetes 2009;58:1634–1640
11. Azad N, Emanuele NV, Abraira C, Henderson WG, Colwell J, Levin SR, Nuttall FQ, Comstock JP, Sawin CT, Silbert C, Rubino FA. The effects of intensive glycemic control on neuropathy in the VA cooperative study on type II diabetes mellitus (VA CSDM). J Diabetes Complications 1999;13:307–313
12. Sullivan KA, Lentz SI, Roberts JL Jr, Feldman EL. Criteria for creating and assessing mouse models of diabetic neuropathy. Curr Drug Targets 2008;9:3–13
13. Keren P, George J, Keren G, Harats D. Non-obese diabetic (NOD) mice exhibit an increased cellular immune response to glycated-LDL but are resistant to high fat diet induced atherosclerosis. Atherosclerosis 2001;157:285–292
14. Petro AE, Cotter J, Cooper DA, Peters JC, Surwit SJ, Surwit RS. Fat, carbohydrate, and calories in the development of diabetes and obesity in the C57BL/6J mouse. Metabolism 2004;53:454–457
15. Huo Y, Winters WD, Yao DL. Prevention of diet-induced type 2 diabetes in the C57BL/6J mouse model by an antidiabetic herbal formula. Phytother Res 2003;17:48–55
16. Hull RL, Andrikopoulos S, Verchere CB, Vidal J, Wang F, Cnop M, Prigeon RL, Kahn SE. Increased dietary fat promotes islet amyloid formation and β-cell secretory dysfunction in a transgenic mouse model of islet amyloid. Diabetes 2003;52:372–379
17. Obrosova IG, Ilnytska O, Lyzogubov VV, Pavlov IA, Mashtalir N, Nadler JL, Drel VR. High-fat diet induced neuropathy of pre-diabetes and obesity: effects of "healthy" diet and aldose reductase inhibition. Diabetes 2007;56:2598–2608
18. Su Y, Liu XM, Sun YM, Jin HB, Fu R, Wang YY, Wu Y, Luan Y. The relationship between endothelial dysfunction and oxidative stress in diabetes and prediabetes. Int J Clin Pract 2008;62:877–882
19. Chen XP, Xun KL, Wu Q, Zhang TT, Shi JS, Du GH. Oxidized low density lipoprotein receptor-1 mediates oxidized low lipoprotein-induced apoptosis in human umbilical vein endothelial cells: role of reactive oxygen species. Vascul Pharmacol 2007;47:1–9
20. Kelly KJ, Wu P, Patterson CE, Temm C, Dominguez JH. LOX-1 and inflammation: a new mechanism for renal injury in obesity and diabetes. Am J Physiol Renal Physiol 2008;294:F1136–F1145
21. Li L, Sawamura T, Renier G. Glucose enhances human macrophage LOX-1 expression: role for LOX-1 in glucose-induced macrophage foam cell formation. Circ Res 2004;94:892–901
22. Mehta JL, Chen J, Yu F, Li DY. Aspirin inhibits ox-LDL-mediated LOX-1 expression and metalloproteinase-1 in human coronary endothelial cells. Cardiovasc Res 2004;64:243–249
23. Pittenger GL, Mehrabyan A, Simmons K, Amandarice, Dublin C, Barlow P, Vinik AI. Small fiber neuropathy is associated with the metabolic syndrome. Metab Syndr Relat Disord 2005;3:113–121
24. Smith AG, Russell J, Feldman EL, Goldstein J, Peltier A, Smith S, Hamwi J, Pollari D, Bixby B, Howard J, Singleton JR. Lifestyle intervention for pre-diabetic neuropathy. Diabetes Care 2006;29:1294–1299
25. Vincent AM, Russell JW, Sullivan KA, Backus C, Hayes JM, McLean LL, Feldman EL. SOD2 protects neurons from injury in cell culture and animal models of diabetic neuropathy. Exp Neurol 2007;208:216–227
26. Sullivan KA, Hayes JM, Wiggin TD, Backus C, Su Oh S, Lentz SI, Brosius F 3rd, Feldman EL. Mouse models of diabetic neuropathy. Neurobiol Dis 2007;28:276–285
27. Russell JW, Berent-Spillson A, Vincent AM, Freimann CL, Sullivan KA, Feldman EL. Oxidative injury and neuropathy in diabetes and impaired glucose tolerance. Neurobiol Dis 2008;30:420–429
28. Russell JW, Sullivan KA, Windebank AJ, Herrmann DN, Feldman EL. Neurons undergo apoptosis in animal and cell culture models of diabetes. Neurobiol Dis 1999;6:347–363
29. McMillen TS, Heinecke JW, LeBoeuf RC. Expression of human myeloperoxidase by macrophages promotes atherosclerosis in mice. Circulation 2005;111:2798–2804
30. McPherson PA, Young IS, McKibben B, McEneny J. High density lipoprotein subfractions: isolation, composition, and their duplicitous role in oxidation. J Lipid Res 2007;48:86–95
31. Wiggin TD, Kretzler M, Pennathur S, Sullivan KA, Brosius FC, Feldman EL. Rosiglitazone treatment reduces diabetic neuropathy in STZ treated DBA/2J mice. Endocrinology 2008;149:4928–4937
32. Zhang H, Saha J, Byun J, Schin M, Lorenz M, Kennedy RT, Kretzler M, Feldman EL, Pennathur S, Brosius 3rd FC. Rosiglitazone reduces renal and plasma markers of oxidative injury and reverses urinary metabolite abnormalities in the amelioration of diabetic nephropathy. Am J Physiol Renal Physiol 2008;295:F1071–F1081
33. Pennathur S, Ido Y, Heller JI, Byun J, Danda R, Pergola P, Williamson JR, Heinecke JW. Reactive carbonyls and polyunsaturated fatty acids produce a hydroxyl radical-like species: a potential pathway for oxidative damage of retinal proteins in diabetes. J Biol Chem 2005;280:22706–22714
34. Bae YS, Lee JH, Choi SH, Kim S, Almazan F, Witztum JL, Miller YI. Macrophages generate reactive oxygen species in response to minimally oxidized low-density lipoprotein: toll-like receptor 4- and spleen tyrosine kinase-dependent activation of NADPH oxidase 2. Circ Res 2009;104:210–218
35. Karadeniz G, Acikgoz S, Tekin IO, Tascylar O, Gun BD, Comert M. Oxidized low-density-lipoprotein accumulation is associated with liver fibrosis in experimental cholestasis. Clinics 2008;63:531–540
36. Martinez-Miguel P, Raoch V, Zaragoza C, Valdivielso JM, Rodriguez-Puyol M, Rodriguez-Puyol D, Lopez-Ongil S. Endothelin-converting enzyme-1 increases in atherosclerotic mice: potential role of oxidized low density lipoproteins. J Lipid Res 2008;50:364–375

37. Shiu SW, Tan KC, Wong Y, Leng L, Bucala R. Glycoxidized LDL increases lectin-like oxidized low density lipoprotein receptor-1 in diabetes mellitus. Atherosclerosis 2009;203:522–527

38. Vincent AM, Feldman EL. Can drug screening lead to candidate therapies for testing in diabetic neuropathy? Antioxid Redox Signal 2008;10:387–393

39. Vincent AM, Stevens MJ, Backus C, McLean LL, Feldman EL. Cell culture modeling to test therapies against hyperglycemia-mediated oxidative stress and injury. Antioxid Redox Signal 2005;7:1494–1506

40. Kataoka H, Kume N, Miyamoto S, Minami M, Murase T, Sawamura T, Masaki T, Hashimoto N, Kita T. Biosynthesis and post-translational processing of lectin-like oxidized low density lipoprotein receptor-1 (LOX-1): N-linked glycosylation affects cell-surface expression and ligand binding. J Biol Chem 2000;275:6573–6579

41. Ikemoto S, Takahashi M, Tsunoda N, Maruyama K, Itakura H, Ezaki O. High-fat diet-induced hyperglycemia and obesity in mice: differential effects of dietary oils. Metabolism 1996;45:1539–1546

42. Surwit RS, Feinglos MN, Rodin J, Sutherland A, Petro AE, Opara EC, Kuhn CM, Rebuffe-Scrive M. Differential effects of fat and sucrose on the development of obesity and diabetes in C57BL/6J and A/J mice. Metabolism 1995;44:645–651

43. Wei P, Lane PH, Lane JT, Padanilam BJ, Sansom SC. Glomerular structural and functional changes in a high-fat diet mouse model of early-stage type 2 diabetes. Diabetologia 2004;47:1541–1549

44. Tesfaye S, Chaturvedi N, Eaton SE, Ward JD, Manes C, Ionescu-Tirgoviste C, Witte DR, Fuller JH. Vascular risk factors and diabetic neuropathy. N Engl J Med 2005;352:341–350

45. Keech AC, Mitchell P, Summanen PA, O'Day J, Davis TM, Moffitt MS, Taskinen MR, Simes RJ, Tse D, Williamson E, Merrifield A, Laatikainen LT, d'Emden MC, Crimet DC, O'Connell RL, Colman PG. Effect of fenofibrate on the need for laser treatment for diabetic retinopathy (FIELD study): a randomised controlled trial. Lancet 2007;370:1687–1697

46. Ando K, Fujita T. Role of lectin-like oxidized low-density lipoprotein receptor-1 (LOX-1) in the development of hypertensive organ damage. Clin Exp Nephrol 2004;8:178–182

47. Vincent AM, Edwards JL, Sadidi M, Feldman EL. The antioxidant response as a drug target in diabetic neuropathy. Curr Drug Targets 2008;9:94–100

48. Thum T, Borlak J. Lox-1 receptor blockade abrogates OXLDL induced oxidative DNA damage and prevents activation of the transcriptional repressor OCT-1 in human coronary arterial endothelium. J Biol Chem 2008;283:19456–19464

49. Ziegler D, Ametov A, Barinov A, Dyck PJ, Gurieva I, Low PA, Munzel U, Yakhno N, Raz I, Novosadova M, Maus J, Samigullin R. Oral treatment with alpha-lipoic acid improves symptomatic diabetic polyneuropathy: the SYDNEY 2 trial. Diabetes Care 2006;29:2365–2370

50. Dandapat A, Hu C, Sun L, Mehta JL. Small concentrations of oxLDL induce capillary tube formation from endothelial cells via LOX-1-dependent redox-sensitive pathway. Arterioscler Thromb Vasc Biol 2007;27:2435–2442

51. Cotter MA, Cameron NE. Effect of the NAD(P)H oxidase inhibitor, apocynin, on peripheral nerve perfusion and function in diabetic rats. Life Sci 2003;73:1813–1824